Thermomechanical behavior of Glulam-beam connected to CLT-wall assemblies with steel doweled connections before, during and after fire

Received 18 February 2022
Revised 10 August 2022
4 October 2022
Accepted 14 October 2022

Milad Shabanian
Department of Standards and Analytics, Insurance Institute for Business and Home Safety Research Center, Richburg, South Carolina, USA and Department of Civil Engineering, University of North Carolina at Charlotte, Charlotte, North Carolina, USA, and
Nicole Leo Braxtan
Department of Civil and Environmental Engineering, University of North Carolina at Charlotte, Charlotte, North Carolina, USA

Abstract

Purpose – Thermomechanical behavior of intermediate-size beam-to-wall assemblies including Glulam-beams connected to cross-laminated timber (CLT) walls with T-shape steel doweled connections was investigated at ambient temperature (AT) and after and during non-standard fire exposure.

Design/methodology/approach – Three AT tests were conducted to evaluate the load-carrying capacity and failure modes of the assembly at room temperature. Two post-fire performance (PFP) tests were performed to study the impact of 30-min (PFP30) and 60-min (PFP60) partial exposure to a non-standard fire on the residual strength of the assemblies. The assemblies were exposed to fire in a custom-designed frame, then cooled and loaded to failure. A fire performance (FP) test was conducted to study the fire resistance (FR) during non-standard fire exposure by simultaneously applying fire and a mechanical load equal to 65% of the AT load carrying capacity.

Findings – At AT, embedment failure of the dowels followed by splitting failure at the Glulam-beam and tensile failure of the epoxy between the layers of CLT-walls were the dominant failure modes. In both PFP tests, the plastic bending of the dowels was the only observed failure mode. The residual strength of the assembly was reduced 14% after 30 min and 37% after 60 min of fire exposure. During the FP test, embedment failure of timber in contact with the dowels was the only major failure mode, with the maximum rate of displacement at 51 min into the fire exposure.

Originality/value – This is the first time that the thermomechanical performance of such an assembly with a full-contact connection is presented.

Keywords Beam-to-wall connection, Mass timber structures, Load-carrying capacity, Residual strength, Fire-resistance, Non-standard fire test

Paper type Research paper

Highlights

(1) Load-carrying capacity of a Glulam-beam connected to CLT-wall headers with T-shape steel doweled connections at ambient temperature (AT) presented.

Journal of Structural Fire Engineering
Vol. 14 No. 3, 2023
pp. 365-384
Emerald Publishing Limited
2040-2317
DOI 10.1108/JSFE-02-2022-0007

(2) Residual strength of the assembly after 30 and 60 min partially exposed to a non-standard fire highlighted.

(3) Fire resistance of the loaded assembly partially exposed to a non-standard fire emphasized.

(4) The failure modes of the assembly before, during, and after non-standard fire tests provided.

Graphical Abstract

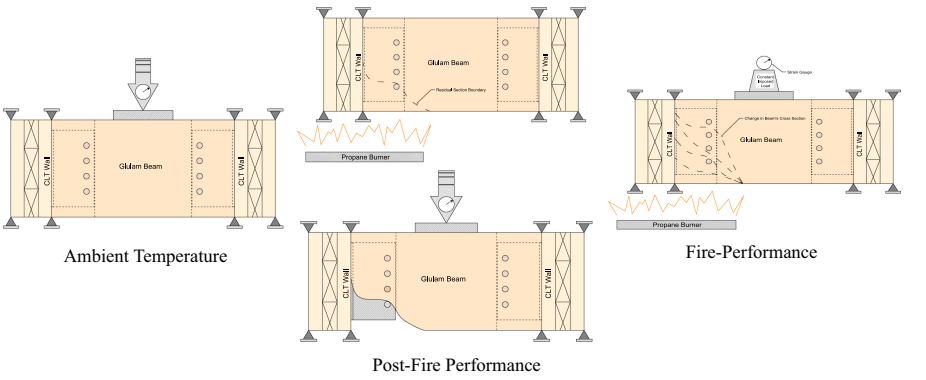

1. Introduction

The application of engineered wood products such as cross-laminated timber (CLT) and Glulam has increased significantly in Europe and more recently in North America (Manninen, 2014; Espinoza *et al.*, 2016; Brandner *et al.*, 2016; Pei *et al.*, 2016; Laguarda-Mallo and Espinoza, 2018; Pierobon *et al.*, 2019). In comparison to the other types of construction materials, engineered wood products provide advantages in architectural appeal, constructability, sustainability and cost, encouraging engineers to design tall timber structures again (Smith and Frangi, 2008; Salvardori, 2017; Kuzmanovska *et al.*, 2018). It is very common to use CLT as large dimensional walls and floor panels in low- to mid-rise panelized construction. Similar to platform framing systems, bearing type of connections with acceptable fire performance (FP) are common in CLT panelized construction. However, due to the complications with accumulative shrinkage, it is challenging to employ CLT panelized construction for high-rise structures (Green and Karash, 2012). On the other hand, current studies confirm the feasibility of using the concept of balloon framing and post and beam construction to reach higher elevations with engineered wood products (Smith and Frangi, 2008; Waugh *et al.*, 2010; Green and Karash, 2012; Salvadori, 2017; Ramage *et al.*, 2017). In this type of construction, columns and beams are usually fabricated from Glulam, walls and floors are CLT, and connections are a combination of bearing, shear and moment-resisting. As has been well-documented in other types of structures, connections play a crucial role in providing integrity, stability and ductility of contemporary high-rise timber structures.

Historically, a wide range of connections has been used for timber structures (Perkins *et al.*, 1933). These connections are usually constructed from metal or wood. Metal connections are one of the most common types of connections employed in heavy timber construction. They increase the ductility and improve the seismic performance of the structure (Buchanan *et al.*, 2001; Fragiacomo *et al.*, 2011; Jorissen and Fragiacomo, 2011; Blaß and Schädle, 2011; Dorn *et al.*, 2013; Gavric *et al.*, 2015), while in a fire incident, they may lose strength and stiffness, and deform considerably (Carling, 1989; Peng *et al.*, 2010; Maraveas *et al.*, 2015). Accordingly, it is essential to study the behavior of metal connections in timber structures during and after a fire incident. The FP of metal connections in timber structures is a function of several variables such as fire exposure time and severity, thermomechanical material properties, and geometry of the connected components, magnitude and direction of the imposed mechanical load, and boundary conditions.

A wide range of studies have been conducted to investigate the FP of metal connectors in timber structures. Most of these studies focused on FP of the connections between members loaded parallel to the grain (Norén, 1996; Lau, 2006; Moss *et al.*, 2008; Frangi *et al.*, 2010; Racher *et al.*, 2010; Audebert *et al.*, 2012; Khelifa *et al.*, 2014). Only a limited number of studies covered FP of Glulam beam-to-beam and beam-to-column connections with beam members loaded perpendicular to the grain (Oksanen *et al.*, 2005; Palma, 2016; Hofmann *et al.*, 2016) and CLT floor-to-floor and floor-to-floor connections (Suzuki *et al.*, 2016; Mahr *et al.*, 2020; Liu and Fischer, 2022; Xing *et al.*, 2022). These fire experiments were mostly performed in closed furnaces with accessibility restrictions, following standard fire curves (ASTM-E119, 2018; EN, 1995-1-2, 2004) which neglect the decay phase of a real fire incident (Gales *et al.*, 2021) and are prescribed for constructions designed using prescriptive building codes. However, contemporary high-rise timber structures with varying exposed combustible timber material should follow a performance-based design procedure. For this purpose, a range of design fires including the standard fire curves should be considered. The fire load is important as it will impact the charring rate and load-carrying capacity of the timber elements.

This paper describes a series of experiments developed and conducted to investigate the performance of Glulam-girder to CLT-wall assemblies connected with T-shape slotted-in doweled connections before, during and after non-standard fire exposure. Experiments were designed considering the restrictions imposed by standard fire tests, previous studies on FP of different connections and the increasing demand for the use of CLT as a vertical, principal structural member.

2. Research motivation

Timber assemblies loaded perpendicular to grain are vulnerable to brittle splitting failure mode. An experimental study performed on Glulam beam-to-column assemblies connected with slotted-in doweled connections (Palma, 2016) confirmed this issue. In this study, increasing the gap from 10 mm to 20 mm did not impact the failure mechanism at AT. According to the experiments conducted in this research, reducing the gap will improve the FP of the assembly exposed to the standard fire curve.

Experimental testing on Glulam beam-to-girder assemblies connected with slotted-in doweled connections (Shabanian and Braxtan, 2022) showed that ductility of the dowels plays a vital role in avoiding the splitting failure. This study also illustrated that removing the gap between connecting members will cause a premature splitting failure and reduce in the load carrying capacity of the assembly at AT. Results showed that embedment failure was the dominant failure mode on the beam side, and splitting failure was the main failure mode on the girder side. The non-standard fire experiments conducted in this research highlighted the impact of timber elements' mass loss and change in geometry on FP of the assembly. This research also studied the post-fire performance (PFP) of Glulam beam-to-girder assemblies

after non-standard fire exposure. In these experiments, embedment failure of the Glulam-beams and plastic bending of the dowels occurred before the splitting failure of the Glulam-girders.

The current study considers Glulam-beam to CLT-wall assemblies. Modern mid-to high-rise timber panelized construction often relies on balloon framing wherein the CLT-walls are continuous over two to three stories and floor beams are hung from the wall panels. This is fundamentally different from the bearing type connections previously designed for use in platform construction of low-rise timber structures. Additionally, due to its architectural appeal, CLT-wall panels are often left exposed – which contributes to the potential fire load in a structure. The change in grain orientation of CLT-wall panels will also change the failure mechanism. In the beam-to-girder assembly, the girders were loaded perpendicular to the grain and experienced brittle failure. It is assumed that using CLT-wall for the headers where the laminations are vertically oriented, as in Figure 1, will change the failure mechanism.

Additionally, an experimental study performed on behavior of steel to CLT-wall connection showed that screwed connections performed with high ductility (Hassanieh *et al.*, 2016).

3. Experimental set-up and material properties

Experimental testing was performed on Glulam-beam to CLT-wall assemblies to determine the AT strength of the connection, the residual strength of the connection after fire (PFP) and the strength of the connection during fire (FP). In total, six tests were performed: three at AT, two post-fire and one during fire.

3.1 Assembly description

Experiments were performed on symmetric, intermediate-size assemblies, consisting of two 3-ply CLT-walls connected to a Glulam-beam with two T-shape steel doweled connectors. Table 1 and Figure 2 provide additional details of the assembly.

3.2 Material properties

3.2.1 Cross-laminated timber (CLT). The headers of the assemblies were constructed from 3-ply CLT panels, consisting of three orthogonal layers of graded sawn lumber (spruce–pine–fir)

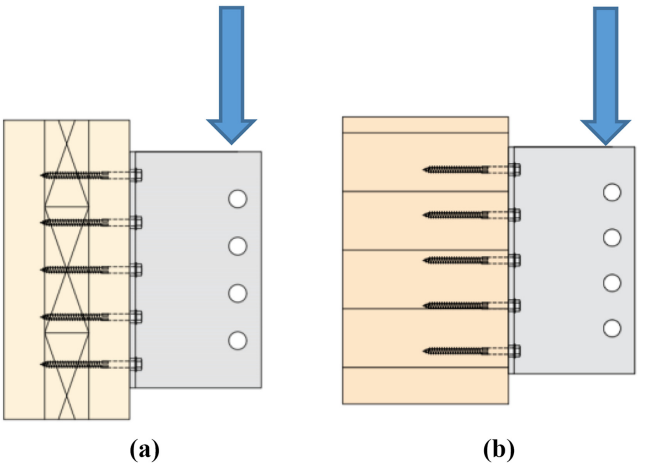

Figure 1.
(a) CLT-wall header vs (b) Glulam-girder header layout in comparison to the load direction

laminated with structural adhesives. The panel moisture content (MC) was approximately 12% (±2%), and density was 515 kg/m^3. The outside layers of the CLT panels were oriented vertically to simulate the CLT layout for a typical wall condition. Table 2 provides the allowable design capacities of the CLT-wall panel loaded parallel to the outermost layer.

3.2.2 Glued-laminated timber (Glulam). In each assembly, the Glulam-beam consisted of small wood laminations of spruce, pine and fir species (90% black spruce) bonded together in parallel using structural adhesives. The Glulam-beams had an average moisture content of 12% and density of 560 kg/m^3. Table 3 shows the design capacities of the Glulam-beams.

3.2.3 Steel connection. The custom designed T-shape slotted-in welded steel doweled connection were fabricated from 7-gauge (4.762 mm) ASTM A572 Grade 50 structural steel with 3.175 mm full-length fillet weld on both sides (ASTM A572, 2018). Figure 3 details the geometry of the connection. Steel connections were welded in US by an AISC certificated steel fabrication company and in accordance with AWC D1.1.

3.2.4 Steel dowels and fasteners. Figure 4 shows the steel dowels and screws in relation to the dimension of the CLT-wall headers and the Glulam-beam. The 114.3 mm length dowels are cut from 12.7 mm structural steel rods (ASTM A572 Gr 50). The 6.35 mm diameter heavy-duty hexagonal connector screws with 76.2 mm length and 50.8 mm thread were manufactured from low-carbon steel wire, grade 1022. This fastener has 1,130 MPa bending strength, 6.36 kN allowable tensile strength and 3.5 kN allowable shear strength.

3.3 Experimental set-up

Plate 1, Figure 5 and 6 show the experimental setup for the AT, PFP and FP tests performed on the Glulam-beam to CLT-wall connections. AT experiments considered only mechanical load on the assembly that was imposed by a SATEC uniaxial testing machine (UTM), PFP tests considered sequential (uncoupled) thermal and mechanical loading, and FP tests considered coupled thermal and mechanical loading. PFP tests were performed after 30 (PFP30) and 60 (PFP60) min of nonstandard fire loading. FP tests were performed with a constant load applied, equivalent to 65% of the AT capacity of the assembly, along with a nonstandard fire exposure. Additional detailed information on the test set-up is provided in related research (Shabanian and Braxtan, 2022).

Figures 7 and 8 show the location of k-type thermocouples in the fire exposed area of the connection for the PFP and FP tests, respectively. In this study, thermocouples (TCs) were glued to the steel connection with Omega thermally conductive epoxy after they were positioned by connection screws in cases where the mechanical connection to the screws was insufficient to hold the TC in place.

During all the fire tests, the CLT-wall was only exposed on the connection side (1-sided exposure), while the Glulam-beam was exposed on 3 sides. The ignition source of the non-standard fire tests was a gas burner built in accordance with NFPA 289 with a nominal 305 mm by 305 open top surfaces, covered with stainless steel mesh. Each test began with a full propane tank containing 6.8 kg of liquid propane and throughout each test approximately

Parts	Quantity	Material	Dimensions (mm)
Headers	2	3-ply CLT-wall (105-3 s)	241.3 × 101.6 × 457.2 mm
Joist	1	Glulam-beam	241.3 × 140 × 457.2 mm
Hangers	2	Steel connection A572 Gr. 50	Plate A: 114.3 × 190.5 × 4.76 mm Plate B: 101.6 × 190.5 × 4.76 mm
Dowels	2 × 4	Steel A572 Gr. 50	D = 12.7 mm, L = 114.3 mm
Screws	2 × 20	Low-carbon steel wire, grade 1022	D = 6.35 mm, L = 76.2 mm

Table 1. Parts consisting of the Glulam-beam to CLT-wall assembly

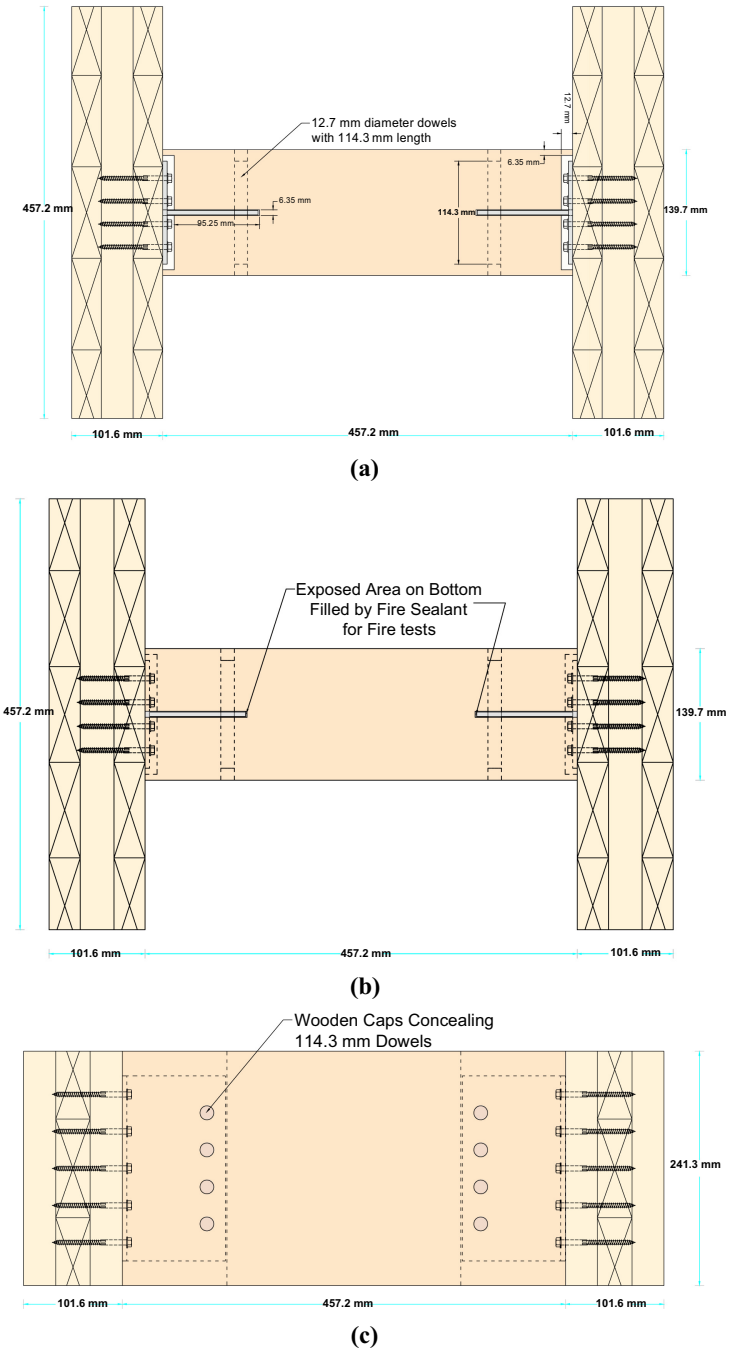

Figure 2.
Assembly geometry: (a) top view, (b) bottom view and (c) front view

CLT stress grade	E1
Orientation	Layers
Species combination	Longitudinal
Stress class	S-P-F
	1950 F_b−1.7E MSR
Bending at extreme fiber, f_b (MPa)	28.2
Longitudinal shear, f_v (MPa)	1.5
Rolling shear, f_s (MPa)	0.5
Compression parallel to grain, f_c (MPa)	19.3
Compression perpendicular to grain, f_{cp} (MPa)	5.3
Tension parallel to the grain, f_t (MPa)	15.4
Modulus of elasticity, E (MPa)	11,700
Shear modulus, G (MPa)	731
Rolling shear modulus, G_s (MPa)	73.1

Table 2.
Material properties of the CLT panel

Stress grade	Bending moment (F_{bx})	Compression perpendicular to grain (Fcpx)	Longitudinal shear (F_{vx})	Compression parallel to grain (F_{vx})	Tension parallel to grain (F_t)	Elastic modulus (E_x)	Specific gravity
24F-ES/NPG	30.7	7.5	2.5	33	20.4	13,100	0.46

Table 3.
Mechanical properties of the Glulam beam (in MPa)

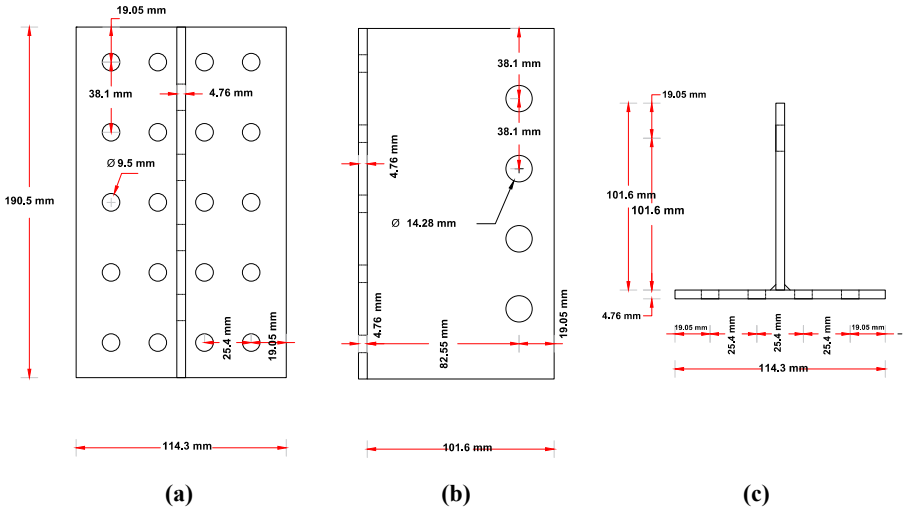

Figure 3.
Geometry of T-shape welded steel connection; (a) front view, (b) side view and (c) top view

4.5 kg of fuel was consumed. The fuel flow was manually controlled in an effort to create consistent fire loads. However, in the absence of an automatic control system, there were slight variations in the intensity of the applied fire load between the tests.

The heating curves of the burner can be approximated bilinearly with an initial heating phase followed by a near constant heating phase. The average burner temperatures during the constant heating phases of the PFP30 and PFP60 tests were 518 °C and 516 °C, respectively, with ranges of 487 °C–570 °C and 496 °C–577 °C, respectively, equating to a variation of applied temperature within 2% between the PFP tests. The constant heating

phase of the FP test had an average temperature of 647 °C and a range of 631 °C–670 °C. Only one FP test was performed, but the average burner temperature in the FP test compared to the PFP tests was approximately 25% higher, which may have led to greater propensity for wood ignition in the assembly in the FP test.

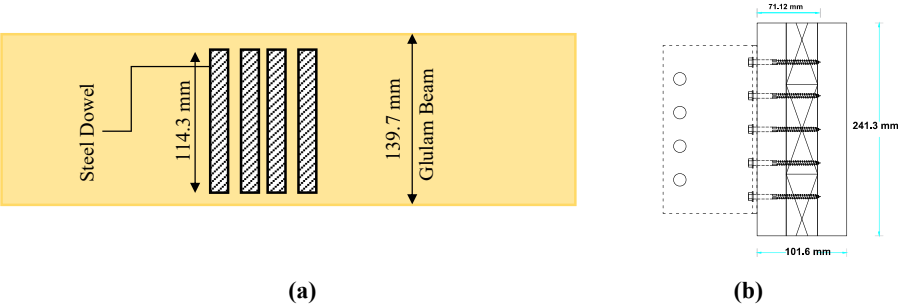

Figure 4.
(a) Steel dowels vs Glulam beam and (b) hexagonal connectors vs 3-ply CLT wall

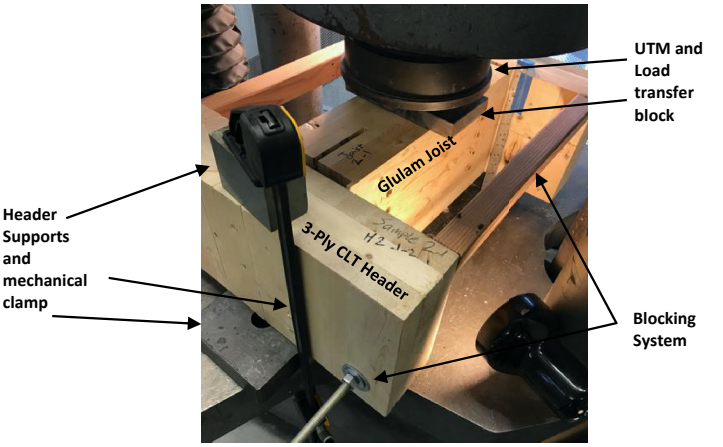

Plate 1.
Test set-up and instrumentation utilized for loading at AT and PFP

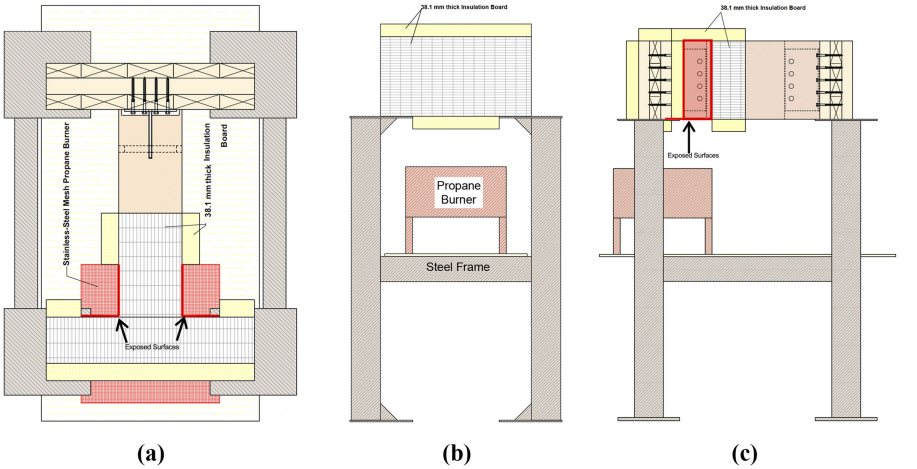

Figure 5.
PFP fire test set-up, (a) top view, (b) side view and (c) front view

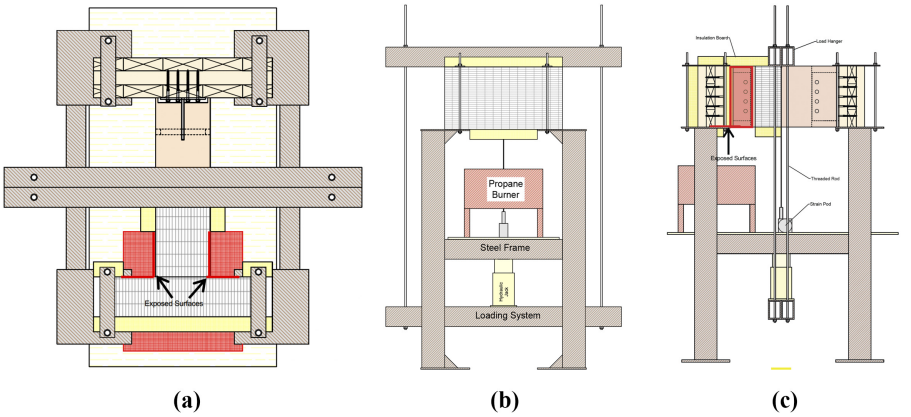

Figure 6.
FP test set-up, (a) top view, (b) side view and (c) front view

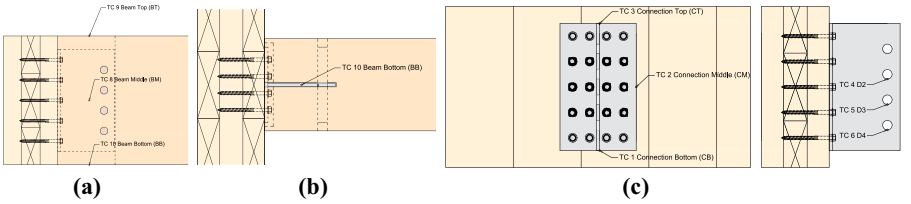

Figure 7.
Thermocouples arrangement for PFP test

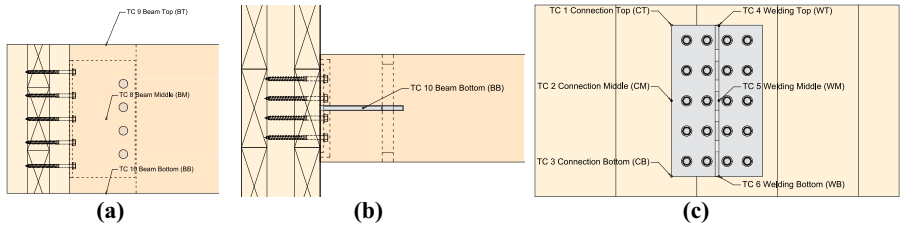

Figure 8.
Thermocouples arrangement for FP test

4. Test results

4.1 Ambient temperature results

Figure 9 shows the load–displacement curves of the Glulam-beam to CLT-wall assemblies tested at AT. The average load-carrying capacity of the assembly was 166.8 kN. According to these curves, the average elastic stiffness of the assembly was approximately 15.5 kN/mm.

Plate 2 shows the failure modes that occurred during AT tests. In all AT tests, failure of the Glulam-beam was initiated by the plastic embedment failure of the Glulam-beam at the dowels' contact locations and continued by plastic bending of the steel dowels (Plate 2a). Tests were stopped after brittle splitting failure occurred close to the top dowels (Plate 2b). It is interesting to notice the importance of having gap between joist and header. In US, load-carrying capacity of hangers in timber structures evaluates in accordance with ASTM D7147 which requires a minimum 1/8-in gap between joist and headers. Metal hanger manufacturers evaluate their products by this standard while providing recommendations to remove the gap for better FP. On the CLT-walls, the tensile withdrawal force of the screws near the top half of the assembly resulted in a tensile plug-out between the CLT-wall layers (Plate 2c). However, this failure may not occur in taller CLT-wall panels with more resistance against tension.

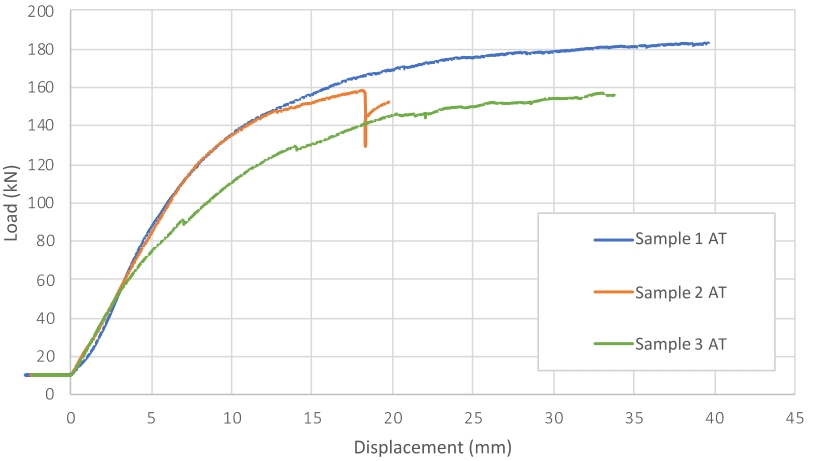

Figure 9.
Load-displacement of the Glulam-beam to CLT-wall assembly at ambient temperature (AT)

Plate 2.
Ambient temperature failure modes (a) ductile embedment failure and bending of the dowels, (b) brittle splitting failure and (c) plug-out tensile failure of the CLT-wall

4.2 Post-fire performance results

Two PFP tests were conducted to study the degradation in residual load-carrying capacity of the Glulam-beam to CLT-wall assembly exposed to 30- and 60-min non-standard fires. In both experiments, the temperature of the burner increased during the first five minutes and then was held constant near 540 °C. The temperature of the burner can be compared to the ASTM E119 standard fire curve in Figure 10. The ASTM fire also reaches 540 °C in the first five minutes, but then continues to slowly increase for the duration of the fire loading. At 30 min fire duration, the ASTM E1119 fire reaches 845 °C, approximately 50% higher than the burner temperature reached in this research. Also, of note is the addition of fire sealant to the 60-min test assembly. Results of these tests included measurements of the heat distribution during the fire tests and the midspan load–displacement behavior of the burnt samples during the loading phase.

Figure 10 shows the PFP heat distribution for the 30-min fire (PFP30) without the fire sealant. Thermocouples 1, 2 and 3 (TC1, TC2 and TC3) recorded the temperature at the bottom, middle and top of the steel connection, respectively. As it was expected, TC1 recorded the highest temperature in the steel connection. After 30 min of fire exposure, the maximum connection temperature occurred in the bottom of the connection (375 °C), while the minimum recorded temperature was at the top of the connection (75 °C). According to the former studies (Lee *et al.*, 2012; Sajid and Kiran, 2019), the post-fire mechanical

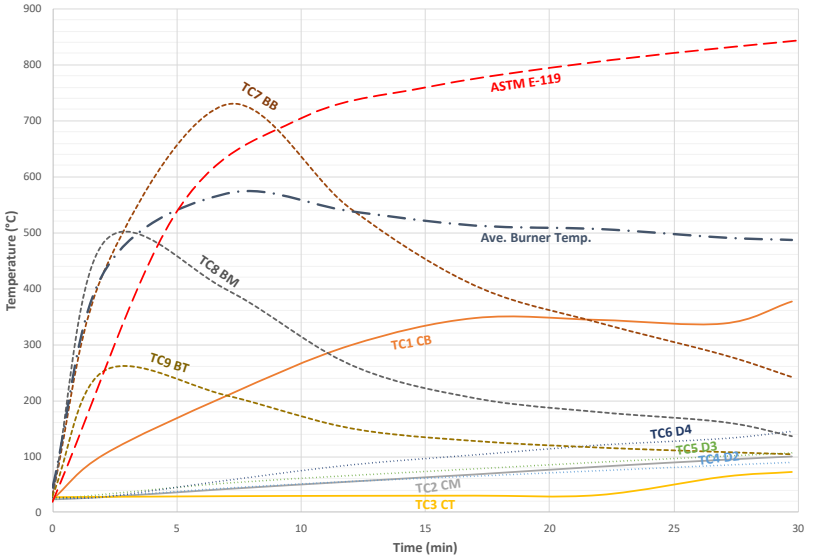

Figure 10.
PFP30 heat distribution along the exposed area

properties of ASTM A572 Gr 50 remain unaffected after exposure to temperatures up to 600 °C. Hence, no reduction in residual strength of the steel connection is expected. Temperatures of the steel connection at the point of contact with the three lower dowels were also recorded by TC4, TC5 and TC6. These temperatures followed the same increasing pattern as the other parts of steel connection. TC4, located closer to the beam bottom, had the highest temperature (145 °F) of the temperatures recorded at the lower dowels.

Thermocouples TC7, TC8 and TC9 measured the Glulam-beam temperatures at the bottom, middle and top of the beam. The Glulam-beam temperature increased at first then decreased during the combustion when the beam's surface began to decay. Based on the visual observations, the Glulam-beam ignited after 1 min on the exterior sides and after 2 min on the bottom. The beam temperatures recorded by TC7 and TC8 confirm ignition as the data as temperatures begin to exceed the temperature of the burner and reach the ignition temperature of wood at approximately 2 min into the test and 300 °C. Plate 3 shows the assembly during and after 30 min fire exposure. At the end of this experiment, the average temperature of the exposed beam was 155 °C when exposed to the nearly constant 540 °C. It is assumed that exposure to the higher intensity ASTM E119 fire would lead to greater beam temperatures and more extensive charring.

Figure 11 shows the heat distribution of the assembly exposed for 60 min to the prescribed fire (PFP60). The figure also shows the continually increasing ASTM E119 fire, which reaches 930 °C at 1-h fire duration in contrast to the nearly constant burner temperature of 540 °C. Similar to the PFP30 test, the Glulam-beam bottom ignited when the beam temperature reached the wood ignition temperature of 300 °C. In this case, the maximum temperature experienced by the beam was 775 °C. The decay phase on the beam's surface fire began after 12 min, and the resulting beam temperatures decreased. TC1 recorded the highest temperatures along the steel connection, and after 60 min of fire exposure, the maximum temperature in the bottom of the connection was 430 °C.

Plate 3.
Glulam-beam to CLT-wall (a) test set-up (b) during and (c) after PFP30 fire test

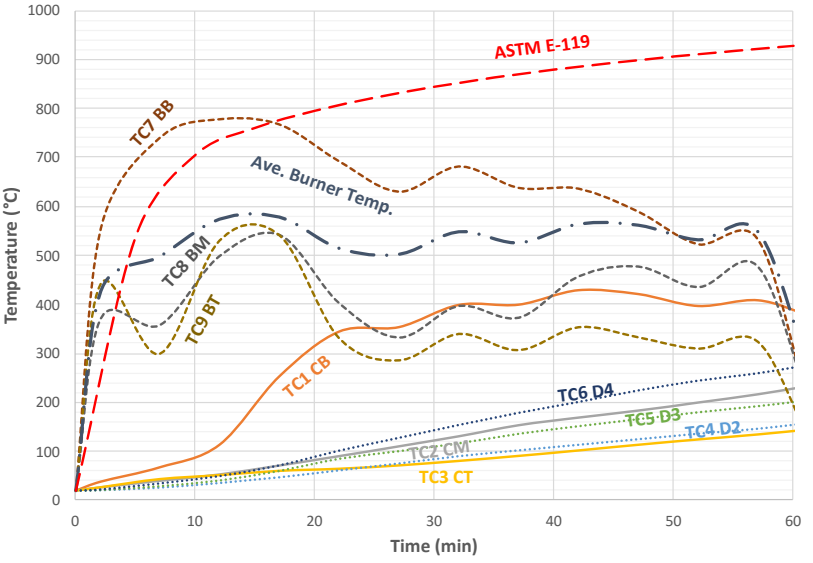

Figure 11.
PFP60 heat distribution along the exposed area

Consequently, the fire exposure did not impact the residual strength of the steel connection after cooling. The fire-sealant had a considerable impact on the temperature of the connection for the first 12 min of the fire, and then the temperature in the connection began to increase more rapidly. Finally, at the end of this experiment, the average temperature of the beam at the exposed area to the non-standard fire was 270 °C and 640 °C less than ASTM E−119. At the end of this experiment, the average temperature of the exposed beam was 275 °C when the temperature of the burner was 380 °C.

Plate 4 shows the Glulam-beam to CLT-wall assembly during and after the PFP60 fire test. While the temperature in the connection began to increase after 12 min of fire more rapidly, Plate 4c shows that the fire sealant stays in place until the end of fire experiment insulating

the connection from the heat. During both fire tests, the temperature of the beam increased due to the consumption of the combustible timber fuel while temperature of the connection increased as it was exposed more due to the progress in charring.

According to Figure 12, the residual load-carrying capacity of the assembly after 30 min of fire exposure was reduced to 144.56 kN (86% of the ambient capacity). The embedment failure of the beam and plastic bending of the dowels were the dominant captured failure modes.

Figure 12 also shows that the load-carrying capacity of the assembly after 60 min was reduced to 105.4 kN (63% of the ambient capacity). The embedment failure of the beam and plastic bending of the dowels were the main failure modes in this experiment. Since in both tests the steel connection itself is expected to maintain the AT strength, the reduction in load-carrying capacity is likely caused by the loss in gross cross-section of the wood due to the charring and strength reduction in the thermal penetrated zone behind the char layer.

Plate 5 shows the assemblies exposed for 30 and 60 min to the non-standard fire after failure. Extensive charring appears on the heated side of the assembly for both the 30- and 60-

(a) (b) (c)

Plate 4.
(a) Fire sealed Glulam-beam to CLT-wall assembly (b) during and (c) after 60 min PFP test

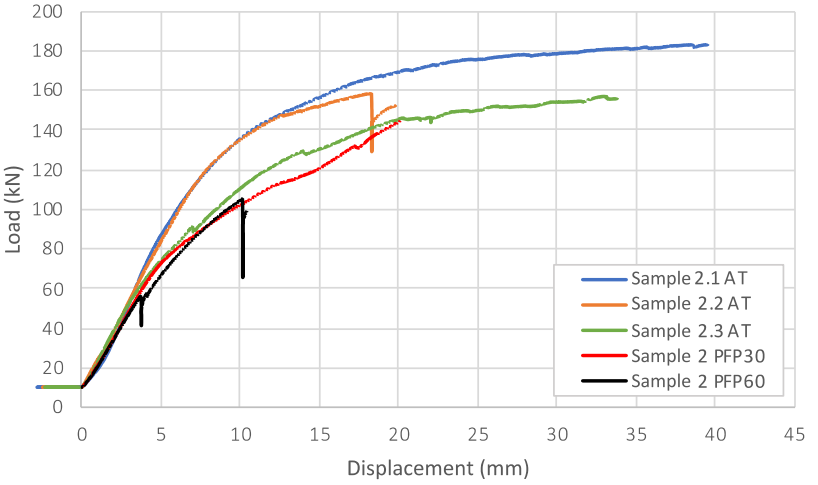

Figure 12.
Load-displacement of Glulam-beam to CLT-wall assembly exposed 30 and 60 min

min PFP tests. The right side of the connection remained unaffected during the PFP tests. In both PFP30 and PFP 60, the premature splitting occurred only on the unexposed side while both sides experienced the embedment failure. This highlights the importance of having gap between members in this type of assemblies. Ultimately, the assemblies failed due to embedment on the fire exposed side of the beam.

4.3 Fire-performance results

The FP tests were conducted to study the fire resistance (FR) of a loaded assembly partially exposed to a non-standard fire. The sample was loaded with a constant downward load of 110 kN at the mid-span of the Glulam-beam during the fire test. Figure 13 shows the heat distribution along the exposed area of the Glulam-beam during the fire test. According to this figure, the Glulam-beam ignited after 2 min. During FP test, the temperature of the burner was held constant at approximately 650 °C. Although, the beam bottom temperature increased up to 760 °C and decreased afterward when the

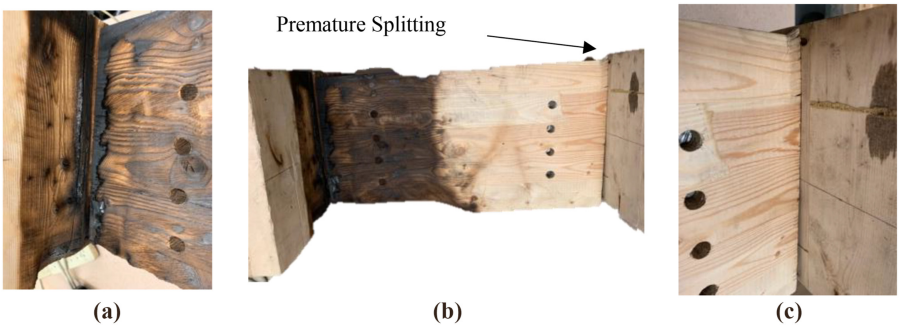

Plate 5.
Glulam-beam to CLT-wall assemblies after loading step; (a) exposed side, (b) PFP30 after loading step and (c) unexposed side

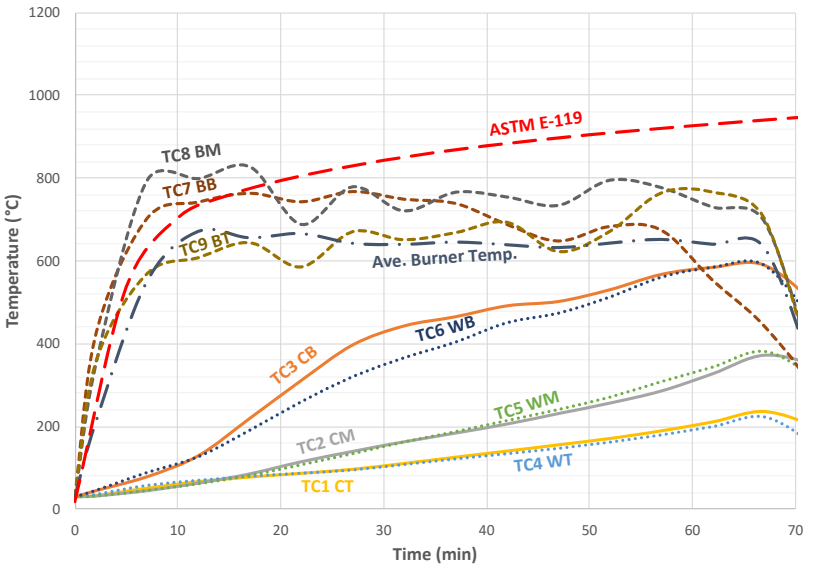

Figure 13.
Heat distribution along the exposed area of the assembly during FP test

beam's surface charred and degraded. The FP test was terminated after 70 min. During this time, the maximum experienced temperature of the steel connection was 590 °C in the bottom of the connection.

According to Figure 14 and based on the visual observation, the maximum displacement of the sample occurred 51 min into the non-standard fire exposure. The maximum rate of displacement occurred at this time, and it was 3 (mm/min). At 51 min into the fire, the average temperature recorded over the steel connection was approximately 480 °C, at this temperature, the steel is expected to maintain 80% of its AT yield strength and 58% of its AT elastic modulus based on Eurocode prescribed reduction factors for the properties of steel at elevated temperatures. While the mechanical properties of the steel connection were degraded, the reserve capacity of the connection prevented failure within the connection itself.

The entire FP test was recorded by a fixed video camera. The recorded videos and captured pictures were used for further investigation on the FP of the assembly. Plate 6 shows video captures of the FP test at different times.

Plate 7 shows the residual section of the Glulam-beam to CLT-wall assembly after the FP test. The embedment failure of the Glulam-beam was the only failure occurred in this assembly. During the FP test, the CLT-wall was exposed to fire only from one side (the side in contact with connection). The char depth on the exposed side was almost equal to the thickness of the surface layer of the CLT (34 mm). This depth was decreased toward the top of CLT-wall member, specifically in contact with the steel connection. Higher temperature of the steel connection in the bottom resulted in deeper char layer. Consequently, due to the change in geometry and boundary condition, the steel connection rotated around the top screws and caused a displacement in the beam member. The displacement of the beam and connection put the top and bottom dowels in more stress. The connection rotation followed by beam displacement stopped when the beam member seated on the top screws. Plate 7 also shows the contact area of the Glulam-beam and change in boundary condition.

5. Discussion and conclusions

This research focused on the performance of Glulam-beam to CLT-wall assemblies connected with T-shaped slotted-in steel connections exposed to mechanical load before, during and after non-standard fire.

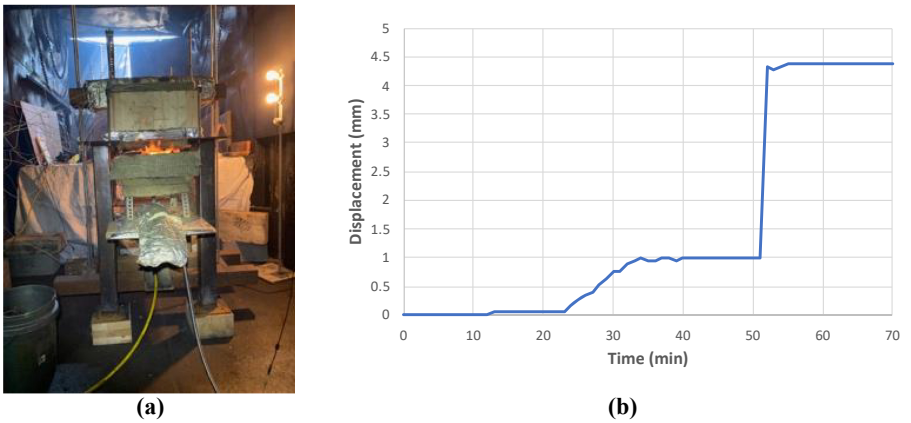

(a) (b)

Figure 14.
(a) FP test set-up, (b) time-displacement at the mid-span of the Glulam-beam

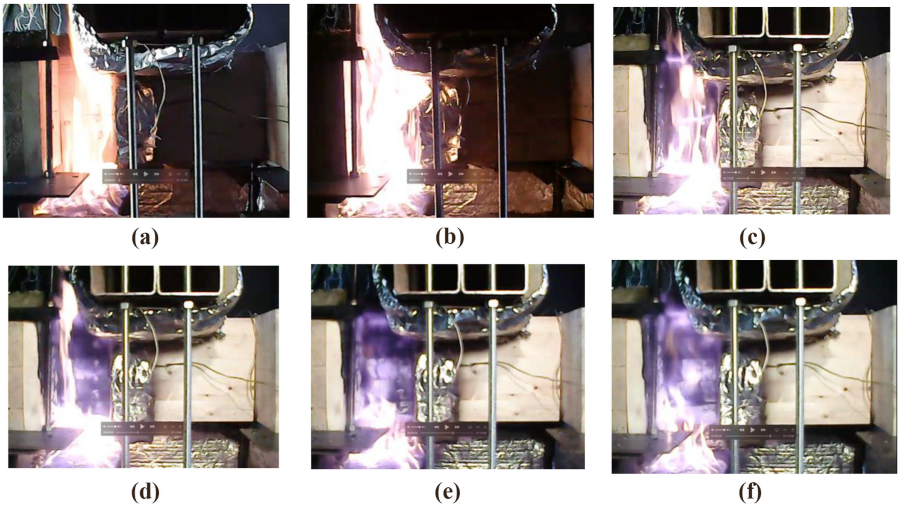

Plate 6.
Fire-performance test video shots;
(a) $t = 1$ min,
(b) $t = 2$ min,
(c) $t = 15$ min,
(d) $t = 30$ min,
(e) $t = 45$ min and
(f) $t = 60$ min

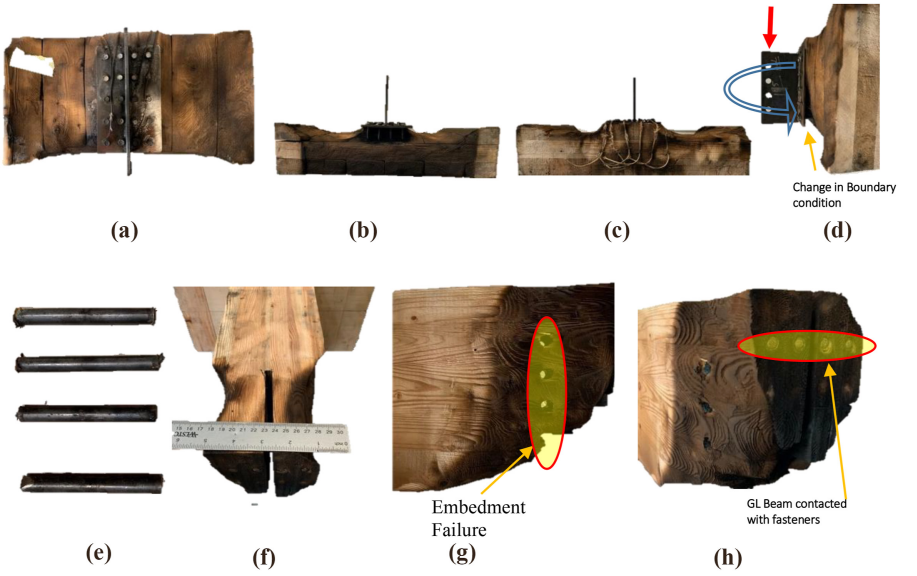

Plate 7.
Residual section of the Glulam-beam to CLT-wall assembly after the fire-performance test; exposed header residual section: (a) front view, (b) lower view, (c) top view, (d) side view, (e) dowels, Glulam-beam residual section: (f) top view, (g) side view, (h) front view

According to the tests performed at AT, the average load-carrying capacity of the assembly was 166.8 kN. The failure of the assembly initiated by the ductile embedment failure of the Glulam-beam, followed by plastic bending of dowels, and ultimately splitting failure of the Glulam-beam occured. Tensile plug-out also occurred in the CLT-wall, but this failure mode may be less likely in an actual wall structure with a greater height than the wall segment tested. The premature type of splitting failure occurred during these experiments due to the friction between sliding surfaces of the beam element on the wall headers. The perpendicular to the grain shear force caused by this friction resulted in splitting failures at the edge and

away from the dowel locations. This is an important finding that highlights the importance of having gap between beam and wall at the connection location. While removing the gap can improve the fire performance of the connection, it has a negative impact on load carrying capacity of the assembly even at AT.

For the assembly loaded after 30 min of non-standard fire exposure (PFP30), the embedment failure of the Glulam-beam and plastic bending of the dowels were main failure modes. The load-carrying capacity of the assembly was reduced by 14% after 30 min fire exposure. The maximum recorded temperature of the steel connection during the PFP30 test was 375 °C. Therefore, the reduction in load-carrying capacity of the assembly is attributed to the loss of wooden members' cross-section and strength in the thermal penetration zone behind the char layer.

The PFP of the assembly exposed to the non-standard fire for 60 min (PFP60) followed the same pattern as the PFP30 specimen. However, the load carrying capacity of the assembly was reduced by 37% after 60 min fire exposure. The maximum recorded temperature of the steel connection during the PFP60 test was 430 °C.

For the loaded assembly tested during the non-standard fire (FP), the imposed load was 65% of the expected load-carrying capacity of the assembly. The ductile embedment failure of the beam was the only observed failure mode. The loaded assembly experienced the maximum displacement after 51 min non-standard fire exposure. The temperature within the connection was 480 °C at 51 min, and although the steel material properties were degraded due to the elevated temperature, the reserve capacity of the connection prevented failure in the connection itself, and the main final failure mode for the assembly was embedment failure in the beam.

The fire sealant utilized for the PFP60 and FP tests protected the steel connection. However, the change in boundary condition and advancing fire surface dictated by charring limited the impact of fire sealant.

Currently, International Building Code 2021, Section 2304.10, requires that the temperature rise at any portion of the connection to be limited to an average temperature rise of 250 °F and a maximum rise of 325 °F, during the ASTM E119 test for the required corresponding FR time of the connection.

During all the fire tests, while the temperature of the burner was lower than the ASTM E119 furnace, the temperature of the connection was higher than the prescribed limitations. However, the increase in temperature did not significantly affect the performance of the connection, and the key parameters in reducing the strength of the assembly were charring, reduction in gross cross-section and strength of the exposed part of the assembly and change in boundary condition. Additionally, it was found that the presence of the steel connection promoted the charring process and facilitated the failure of the wooden beam at the connection area.

Another key observation during the fire tests was enlargement of the fasteners. In all the fire tests, temperature rise in connection resulted in enlargement of the screws which resulted in rotation of the connections. This enlargement in screws can also cause a gap between insulation boards and assembly which is undesirable from protection point of view.

Finally, the CLT-wall to Glulam-beam assembly considered in this research was subject to similar AT, post-fire and FP testing procedure as the Glulam beam-to-girder connection tested by Shabanian and Braxtan (2022). The Glulam-beam and steel connection were the same in both tests, but the headers varied – CLT-wall compared to Glulam-girder – as well as boundary condition and imposed thermal and mechanical loads. In both cases, however, the controlling failure mode occurred in the Glulam-beam despite the altered geometry and orientation of the CLT-wall. Similar trends were observed in the post-fire and FP thermal results as well. As expected, the charring depth in the CLT headers decreased when exposure limited to only one side.

References

ASTM A572/A572M-18 (2018), *Standard Specification for High-Strength Low-Alloy Columbium-Vanadium Structural Steel*, ASTM International, West Conshohocken, PA, available at: www.astm.org

ASTM-E119-18 (2018), *Standard Test Methods for Fire Tests of Building Construction and Materials*, ASTM International, West Conshohocken, PA, doi: 10.1520/D7147-11R18.

Audebert, M., Dhima, D., Taazount, M. and Bouchaïr, A. (2012), "Behavior of dowelled and bolted steel-to-timber connections exposed to fire", *Engineering Structures*, Vol. 39, pp. 116-125.

Blaß, H.J. and Schädle, P. (2011), "Ductility aspects of reinforced and non-reinforced timber joints", *Engineering Structures*, Vol. 33 No. 11, pp. 3018-3026.

Brandner, R., Flatscher, G., Ringhofer, A., Schickhofer, G. and Thiel, A. (2016), "Cross laminated timber (CLT): overview and development", *European Journal of Wood and Wood Products*, Vol. 74 No. 3, pp. 331-351.

Buchanan, A., Moss, P. and Wong, N. (2001), "Ductile moment-resisting connections in glulam beams", *Proceedings of NZSEE Conference*, Wairakei Resort, Taupo, New Zealand.

Carling, O. (1989), *Fire Resistance of Joint Details in Loadbearing Timber Construction: A Literature Survey*, Translated from original Swedish by Harris, B. and Yiu, P.K.A., Building Research Association of New Zealand, Judgeford, BRANZ Study Report SR 18, available at: https://d39d3mj7qio96p.cloudfront.net/media/documents/SR18_Fire_resistance_of_joint_details_in_load_bearing_timber_construction.pdf (accessed 27 December 2021).

Dorn, M., de Borst, K. and Eberhardsteiner, J. (2013), "Experiments on dowel-type timber connections", *Engineering Structures*, Vol. 47, pp. 67-80.

EN 1995-1-2 (2004), *Design of Timber Structures—Part 1-2: General—Structural Fire Design*, European Committee for Standardization, Brussels.

Espinoza, O., Trujillo, V.R., Mallo, M.F.L. and Buehlmann, U. (2016), "Cross-laminated timber: status and research needs in Europe", *BioResources*, Vol. 11 No. 1, pp. 281-295.

Fragiacomo, M., Dujic, B. and Sustersic, I. (2011), "Elastic and ductile design of multi-storey crosslam massive wooden buildings under seismic actions", *Engineering Structures*, Vol. 33 No. 11, pp. 3043-3053.

Frangi, A., Erchinger, C. and Fontana, M. (2010), "Experimental fire analysis of steel-to-timber connections using dowels and nails", *Fire and Materials: An International Journal*, Vol. 34 No. 1, pp. 1-19.

Gales, J., Chorlton, B. and Jeanneret, C. (2021), "The historical narrative of the standard temperature–time heating curve for structures", *Fire Technology*, Vol. 57 No. 2, pp. 529-558.

Gavric, I., Fragiacomo, M. and Ceccotti, A. (2015), "Cyclic behaviour of typical metal connectors for cross-laminated (CLT) structures", *Materials and Structures*, Vol. 48 No. 6, pp. 1841-1857.

Green, M.C. and Karsh, J.E. (2012), *The Case for Tall Wood Buildings: How Mass Timber Offers a Safe, Economical, and Environmentally Friendly Alternative for Tall Building Structures*, MgbArchitecture+ Design, Vancouver, BC.

Hassanieh, A., Valipour, H.R. and Bradford, M.A. (2016), "Load-slip behaviour of steel-cross laminated timber (CLT) composite connections", *Journal of Constructional Steel Research*, Vol. 122, pp. 110-121.

Hofmann, V., Grafe, M., Werther, N. and Winter, S. (2016), "Fire resistance of primary beam–secondary beam connections in timber structures", *Journal of Structural Fire Engineering*, Vol. 7 No. 2, pp. 126-141.

Jorissen, A. and Fragiacomo, M. (2011), "General notes on ductility in timber structures", *Engineering Structures*, Vol. 33 No. 11, pp. 2987-2997.

Khelifa, M., Khennane, A., El Ganaoui, M. and Rogaume, Y. (2014), "Analysis of the behavior of multiple dowel timber connections in fire", *Fire Safety Journal*, Vol. 68, pp. 119-128.

Kuzmanovska, I., Gasparri, E., Monne, D.T. and Aitchison, M. (2018), "Tall timber buildings: emerging trends and typologies", *2018 World Conference on Timber Engineering*.

Laguarda-Mallo, M.F. and Espinoza, O. (2018), "Awareness, perceptions and willingness to adopt CLT by US engineering firms", *BioProducts Business*, Vol. 3 No. 1, pp. 1-14.

Lau, P.H. (2006), "Fire resistance of connections in laminated veneer lumber (LVL)", MEFE thesis, Department of Civil Engineering, University of Canterbury.

Lee, J., Engelhardt, M.D. and Taleff, E.M. (2012), "Mechanical properties of ASTM A 992 steel after fire", *Engineering Journal (Chicago)*, Vol. 49 No. 1, pp. 33-44.

Liu, J. and Fischer, E.C. (2022), "Review of large-scale CLT compartment fire tests", *Construction and Building Materials*, Vol. 318, 126099.

Mahr, K., Sinha, A. and Barbosa, A.R. (2020), "Elevated temperature effects on performance of a cross-laminated timber floor-to-wall bracket connections", *Journal of Structural Engineering*, Vol. 146 No. 9, 04020173.

Manninen, H. (2014), *Long-term Outlook for Engineered Wood Products in Europe*, Technical Report 91, European Forest Institute, Joensuu.

Maraveas, C., Miamis, K. and Matthaiou, C.E. (2015), "Performance of timber connections exposed to fire: a review", *Fire Technology*, Vol. 51 No. 6, pp. 1401-1432.

Moss, P., Fragiacomo, M., Austruy, C. and Buchanan, A. (2008), "On the design of timber bolted connections subjected to fire", 10th World Conference on Timber Engineering (WCTE 2008), Proceedings of the 2008 WCTE, Miyazaki, Japan, 2-5 June 2008, p. 8.

Norén, J. (1996), "Load-bearing capacity of nailed joints exposed to fire", *Fire and Materials*, Vol. 20 No. 3, pp. 133-143.

Oksanen, T., Kevarinmäki, A., Yli-Koski, R. and Kaitila, O. (2005), "Ruostumattomasta teräksestä valmistettujen puurakenteiden liitosten palonkestävyys".

Palma, P. (2016), "Fire behaviour of timber connections", Doctoral Dissertation, ETH Zurich.

Pei, S., Rammer, D., Popovski, M., Williamson, T., Line, P. and van de Lindt, J.W. (2016), "An overview of CLT research and implementation in North America", *WCTE 2016*, Vienna, Austria, August 22-25, 2016.

Peng, L., Hadjisophocleous, G., Mehaffey, J. and Mohammad, M. (2010), "Fire resistance performance of unprotected wood–wood–wood and wood–steel–wood connections: a literature review and new data correlations", *Fire Safety Journal*, Vol. 45 Nos 6-8, pp. 392-399.

Perkins, N.S., Landsem, P. and Trayer, G.W. (1933), *Modern Connectors for Timber Construction*, US Government Printing Office, Washington, DC.

Pierobon, F., Huang, M., Simonen, K. and Ganguly, I. (2019), "Environmental benefits of using hybrid CLT structure in midrise non-residential construction: an LCA based comparative case study in the US Pacific Northwest", *Journal of Building Engineering*, Vol. 26, 100862.

Racher, P., Laplanche, K., Dhima, D. and Bouchaïr, A. (2010), "Thermo-mechanical analysis of the fire performance of dowelled timber connection", *Engineering Structures*, Vol. 32 No. 4, pp. 1148-1157.

Ramage, M., Foster, R., Smith, S., Flanagan, K. and Bakker, R. (2017), "Super Tall Timber: design research for the next generation of natural structure", *The Journal of Architecture*, Vol. 22 No. 1, pp. 104-122.

Sajid, H.U. and Kiran, R. (2019), "Post-fire mechanical behavior of ASTM A572 steels subjected to high stress triaxialities", *Engineering Structures*, Vol. 191, pp. 323-342.

Salvadori, V. (2017), "Tall wood building", Doctoral dissertation, Master Thesis Architecture, Department of Achitecture, TU Wien Politecnico Milano, Milan, Italy.

Shabanian, M. and Braxtan, N.L. (2022), "Thermo-mechanical behavior of Glulam beam-to-girder assemblies with steel doweled connections before, during and after fire", *Journal of Structural Fire Engineering*, Vol. 13 No. 3, pp. 370-390, doi: 10.1108/JSFE-04-2021-0018.

Smith, I. and Frangi, A. (2008), "Overview of design issues for tall timber buildings", *Structural Engineering International*, Vol. 18 No. 2, pp. 141-147.

Suzuki, J.I., Mizukami, T., Naruse, T. and Araki, Y. (2016), "Fire resistance of timber panel structures under standard fire exposure", *Fire Technology*, Vol. 52 No. 4, pp. 1015-1034.

Waugh, A., Wells, M. and Lindegar, M. (2010), "Tall timber buildings: application of solid timber constructions in multi-storey buildings", International Convention of Society of Wood Science and Technology and United Nations Economic Commission for Europe.

Xing, Z., Zhang, J., Zheng, C. and Lu, C. (2022), "Experimental study and finite element analysis on residual carrying capacity of CLT wall-floor angle bracket connections after fire", *Construction and Building Materials*, Vol. 328, 127113.

Corresponding author
Milad Shabanian can be contacted at: mshabani@alumni.uncc.edu